

## The HELIX Drift Chamber Tracker Design and Implementation

---

**K. McBride,<sup>a,\*</sup> P. S. Allison,<sup>a</sup> M. Baiocchi,<sup>b</sup> J. J. Beatty,<sup>a</sup> L. Beaufore,<sup>c</sup>  
D. H. Calderón,<sup>a</sup> A. G. Castano,<sup>c</sup> Y. Chen,<sup>d</sup> S. Coutu,<sup>d</sup> N. Green,<sup>e</sup> D. Hanna,<sup>f</sup>  
H. B. Jeon,<sup>c</sup> S. B. Klein,<sup>g</sup> B. Kunkler,<sup>g</sup> M. Lang,<sup>g</sup> R. Mbarek,<sup>c</sup> S. I. Mognet,<sup>d</sup>  
J. Musser,<sup>g</sup> S. Nutter,<sup>h</sup> S. O'Brien,<sup>f</sup> N. Park,<sup>b</sup> K. M. Powledge,<sup>c</sup> K. Sakai,<sup>c</sup>  
M. Tabata,<sup>i</sup> G. Tarlé,<sup>e</sup> J. M. Tuttle,<sup>c</sup> G. Visser,<sup>g</sup> S. P. Wakely<sup>c</sup> and M. Yu<sup>d</sup>**

<sup>a</sup>The Ohio State University, Dept. of Physics, Columbus, USA

<sup>b</sup>Queen's University, Dept. of Physics, Engineering Physics and Astronomy, Kingston, Canada

<sup>c</sup>University of Chicago, Enrico Fermi Institute, Chicago, USA

<sup>d</sup>Pennsylvania State University, Dept. of Physics, University Park, USA

<sup>e</sup>University of Michigan, Dept. of Physics, Ann Arbor, USA

<sup>f</sup>McGill University, Dept. of Physics, Montreal, Canada

<sup>g</sup>Indiana University, Dept. of Physics, Bloomington, USA

<sup>h</sup>Northern Kentucky University, Dept. of Physics, Geology and Engineering Technology,  
Highland Heights, USA

<sup>i</sup>Chiba University, Dept. of Physics, Chiba, Japan

E-mail: [kmcbride@uchicago.edu](mailto:kmcbride@uchicago.edu)

HELIX (High Energy Light Isotope eXperiment) is a balloon-borne experiment designed to measure the chemical and isotopic abundances of light cosmic-ray nuclei. Detailed measurements by HELIX, especially of  $^{10}\text{Be}$  from  $\sim 0.2$  GeV/n to beyond 3 GeV/n, will provide essential insights into the propagation processes of the cosmic rays. HELIX measures the rigidity of cosmic rays by tracking their deflection in a 1 Tesla magnetic field with its Drift Chamber Tracker (DCT). This high-resolution gas tracking system utilizes 216 sensing wires with diameter 20  $\mu\text{m}$  to provide both bending and non-bending view measurements. The DCT sense wires collect cosmic-ray-induced ionization through a strong electric drift field of 1 kV/cm. Precise monitoring and control of the gas composition and drift field are accomplished with a suite of housekeeping instruments. We present the design and implementation of the DCT and its readout electronics and highlight cosmic-ray muon analysis developments with straight-through tracks.

38th International Cosmic Ray Conference (ICRC2023)  
26 July - 3 August, 2023  
Nagoya, Japan



---

\*Speaker

## 1. Introduction

The High Energy Light Isotope eXperiment (HELIX) is a balloon-borne cosmic-ray detector designed to measure the flux of the isotopes of light nuclei over the energy range from  $\sim 0.2$  GeV/n to  $\sim 3$  GeV/n [1, 2]. The HELIX science program centers around understanding the propagation of cosmic rays within the Galaxy. A primary science goal is to resolve the ‘clock’ isotope  $^{10}\text{Be}$ , that probes the timescale of cosmic-ray propagation within the Milky Way [3]. The HELIX instrument is a magnetic spectrometer utilizing measurements of charge, velocity, and rigidity to resolve beryllium isotopes and other cosmic-ray nuclei on an event-by-event basis. The velocity and charge are measured with a Time-of-Flight (TOF) system and a Ring-Imaging Cherenkov (RICH) detector, and the rigidity is measured with a Drift Chamber Tracker (DCT) installed in the magnetic field region of a superconducting magnet. The first flight for the HELIX program is projected for the spring of 2024 from Kiruna, Sweden. The TOF and RICH components are documented in other publications [4–6]; this contribution focuses on the DCT.

In order to achieve its scientific goals, HELIX mass precision is required to be at the 3% level. The flow-down from this requirement to the tracker rigidity resolution places constraints on the design. Drift chambers meet this rigidity requirement by allowing a high number of track position measurements while keeping the material overburden low in the active region. In addition, the superconducting magnet, which has been used on previous cosmic-ray detectors [7], geometrically constrains the tracker region. Here we discuss the design of the DCT, focusing on meeting the requirements for HELIX science through system hardware, housekeeping sensors, and developed software.

## 2. DCT overview

The DCT tracks cosmic rays via measurements of their ionization trail through a gas-filled volume and inside a strong magnetic field. The charged cosmic ray deflects in the field based on its momentum and charge, or rigidity ( $R = \frac{pc}{Ze}$ ). The HELIX DCT is a custom-designed gas detector in a drift-chamber configuration with a design goal of  $70\mu\text{m}$  tracking resolution in the bending view (discussed below). The ionization electrons created by the passage of a cosmic ray drift under a strong electric field, generated by wires held at high voltage. These electrons create more ionization, called an avalanche, in the near-field region of the electric-field-generating wires. The drifting ions produced in the avalanche can be measured on a grid of wires as induced current pulses. The times of the current pulses, measured with respect to the event trigger time, are used to calculate the drift times and thereby the drift distances.

The primary components of the DCT system are a gas-filled pressurized aluminum vessel, the Drift Chamber Tracker itself, and a housekeeping system. The DCT consists of tracker wires (called ‘sense wires’), high-voltage (drift) field wires and high-voltage shaping strips, the primary FR-4 mechanical structure, and Front-End (FE) filtering and amplification circuits. The drift-field wires and the high-voltage shaping electrodes can be seen in Figure 1 along with the termination mounting boards, and the DCT FR-4 structure. With drift-distance information from all 216 sense wires, the trajectory of the cosmic ray through the DCT can be reconstructed.

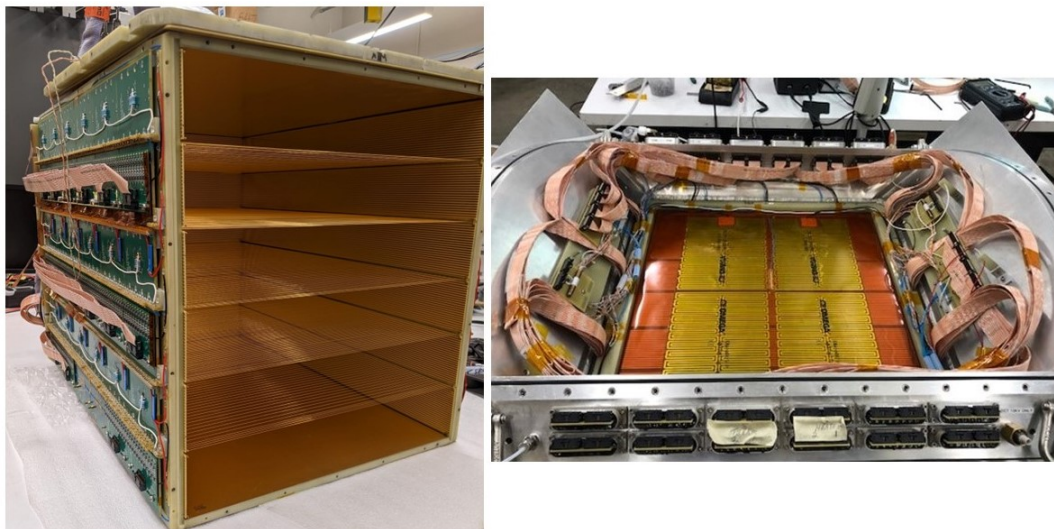


**Figure 1: Left:** A picture of the DCT on its side with its top open, showing 3 drift cells per layer with 2 drift-field wires on either side of the central drift cell. The sense wires are difficult to see and the gold wires that are visible are the drift-field and field-shaping wires. The FEEs for one side of the sense wires are visible on the outer left face. **Right:** A picture of the DCT closed and installed in its vessel. Half of the vacuum-rated feedthroughs for the sense-wire channels appear at the near side of the photo; the other half are on the opposite side. The top section of the DCT is outfitted with heaters, described in Section 5.

Hit positions in the DCT are per sense wire and consist of both a bending and non-bending view coordinate. The bending-view hit is that which is described by the direction of the magnetic field, thus hit positions in this view reconstruct the deflected component of the particle's trajectory. Per sense wire, the induced current from drifting ionization provides a 'drift time' that is transformed to a distance to the sense wire for the bending-view hit position. For the non-bending-view positions, which appear as a straight track, the induced current is measured at both termination ends of each sense wire. This provides a hit position along each sense wire with the charge division method. The reconstruction of the DCT track combines both bending-view and non-bending view measurements using standard tracking algorithms to provide a rigidity measurement.

The DCT offers low material overburden and large acceptance within the existing magnet bore in HELIX. The adjustable parameters in designing the DCT included the number of wires and their separation, the drift-field strength, and the gas physical properties. Many of the challenges with this tracker fundamentally follow from the high-resolution tracking requirement, motivating a precise monitoring and control system of the gas environment and a large number of sense wires.

## 2.1 DCT mechanical

Since HELIX flies at an altitude of  $\sim 40$  km (ambient pressure  $\sim 4$  torr) the tracker is installed in a custom-designed aluminum vessel that withstands the over-pressure of its internal gas held at 1 atm. This vessel includes epoxied vacuum-rated feedthroughs for gas input and output, sense-wire signals, high-voltage wires, and housekeeping cabling. The DCT vessel was proofed to a pressure of 1.5 atm over sea-level ambient (2.5 atm absolute). The tracker component sits inside the vessel on a pair of precision pins such that the vessel and tracker faces are separated to minimize thermal

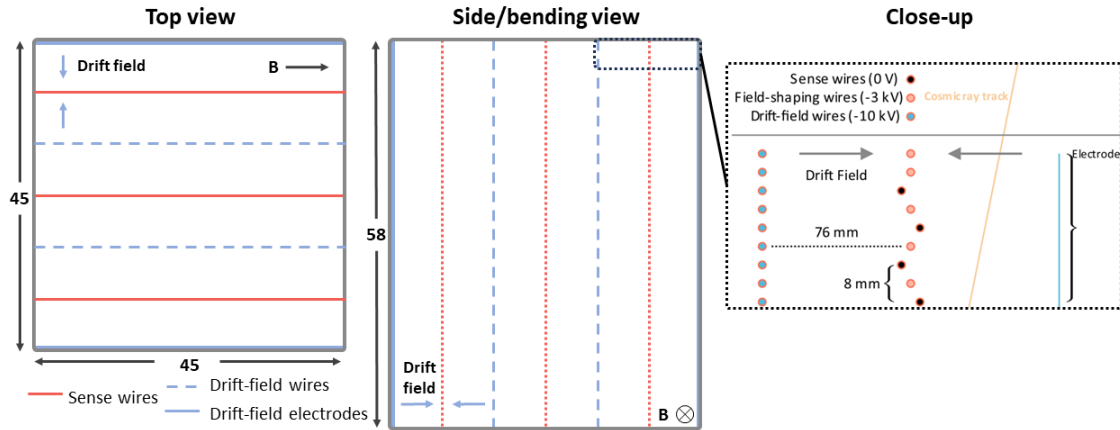


**Figure 2:** **Left:** A diagram of the DCT from the top view, equivalent to the view at left of Figure 1, denoting the layers of wires either as sense or drift-field. **Middle:** The side or bending-view diagram shows the division into 72 layers from top to bottom of 3 drift cells per layer. **Right:** A close-up diagram of the right drift cells with 4 drift cells or sense wires shown. Interspersed with the sense wires in a drift cell are field-shaping wires. The staggering of alternating sense wires appear relative to the field-shaping wires. In the diagrams, the drift field is the reverse direction of the electric field and the units, if not shown, are in cm.

conduction and prevent high-voltage breakdown. The DCT structure has a total FR-4 thickness of 12.7 mm to prevent high-voltage breakdown to the aluminum vessel and eliminate mechanical distortion due to wire tension. The mass of the vessel is about 50 kg and of the DCT itself is 50 kg.

### 3. DCT wires and readout system

The magnet bore provides a physical region for the tracker with dimensions  $500 \times 500 \times 620$  mm<sup>3</sup>. This space provides 72 samples and a maximum drift distance of 76 mm. The DCT consists of drift cells where each cell has a central sense wire. There are 3 drift cells per layer where the central drift cell is spaced 150 mm from the other 2 in the layer. There are 72 layers for a total of 216 drift cells. All wires are strung along the magnetic field direction, at a length of 48 cm. The sense wires are made of *moleculoy* (non-magnetic nickel-chromium alloy,  $4 \Omega/\text{mm}$ ) with a diameter of  $20 \mu\text{m}$ , allowing for a strong electric field for avalanche generation. The wires are strung with a tension of 0.19 N. The sense wire pitch of 8 mm is large compared to the diameter of the wires. To resolve the left-right ambiguity (discussed in Section 4), neighboring layers are alternately staggered in the bending view by 0.3 mm. A close-up view of this stagger is shown at right in Figure 2. The active area of the DCT is  $45 \times 45 \times 58$  cm<sup>3</sup>, utilizing a high fraction of the physical bore region for cosmic-ray tracking.

Interspersed between the sense wires in the drift cell are field-shaping wires held at a lower potential ( $-3$  kV) than the drift-field wires ( $-10$  kV). The wires visible in Figure 1 are both drift-field wires and field-shaping wires, and in between the field-shaping wires are sense wires as shown in the close-up of Figure 2. Figure 2 shows the 3 drift cells in each layer, with drift-field wires on either side of the central drift cell. The drift-field and field-shaping wires are gold-plated aluminum with a diameter of  $250 \mu\text{m}$ . The spacing between the drift-field wires and sense wires is 76 mm, which is the total drift distance. The central drift-cell layer has drift-field wires on either side,

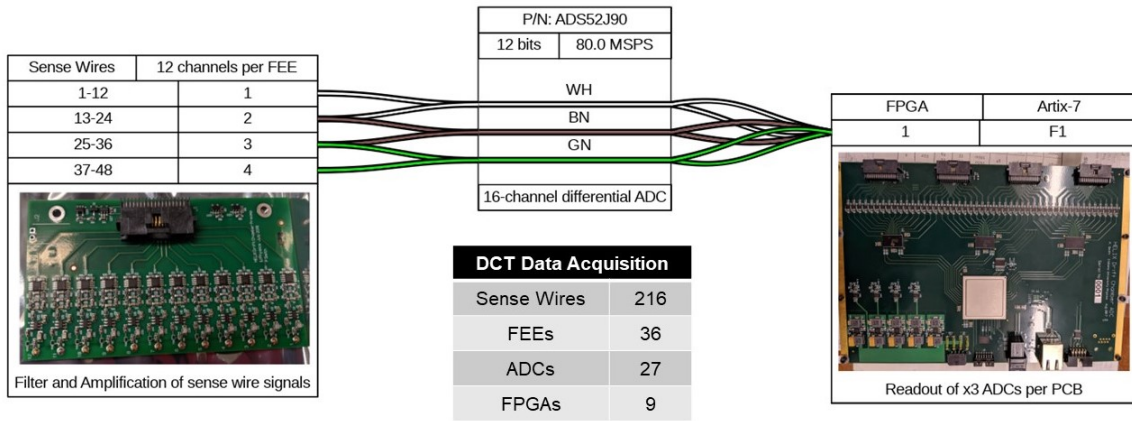


**Figure 3:** Signals on the DCT sense wires are filtered and amplified at the FEEs (left) which take 12 sense-wire signals and make 12 differential pairs that are read out at ADCs (center). Each ADC digitizes 16 sense-wire channels, as shown in the mapping from left to center. The ADC data is recorded with Artix-7 FPGAs housed on the ADC PCBs (right) with 3 ADCs per PCB, or 48 sense wire signals per PCB. The ADCs sample the sense-wire channel for a 10  $\mu$ s window after a trigger, at a rate of 80 MSPS. There are 9 total FPGAs to record the 432 sense-wire signals as each end of the sense wire is measured.

but the 2 non-central drift-cell layers have field-shaping electrodes (see Figure 2). In this way, a near-uniform drift field is created such that ionization electrons on either side of the sense wire in a cell drift at constant velocity. The field-shaping wires contribute to the ionization electrons drifting towards sense wires in a drift cell. A schematic display of the drift cells and drift-field wires is shown in the event display of Figure 4.

The ends of all wires terminate with UV-cured epoxy feedthroughs onto the wire termination mounting boards that are the circuit boards appearing in Figure 1. Wires are positioned on these PCBs within a bridge of machinable glass ceramic (Macor TM) with 50  $\mu$ m precision tolerance. Front-End Electronics (FEEs) boards are attached which provide filtering and amplification of the sense-wire signals. Each FEE board has 12 sense-wire channels which become differential-pair signals that exit the DCT vessel through vacuum-rated feedthroughs. The FEEs implement a transimpedance stage (AD LTC6268), along with a differential driver stage (TI THS4521). After this first stage, channels are routed to 9 analog-to-digital converter (ADC) boards, located in an electronics crate near the vessel, for readout and packaging of data. The ADC PCBs each provide three 16-channel 12-bit ADCs (ADS52J90) sampled at a rate of 80 mega samples per second (MSPS). These ADCs are programmed and interfaced through an Artix-7 field-programmable gate array (FPGA). The 216 sense wires, each measured at both ends, are recorded with the FPGA through the ADCs as 432 voltage waveforms. The first-stage FEEs and the ADC PCBs are shown in Figure 3 which includes the 12-channel FEE to 16-channel ADC mappings.

#### 4. DCT tracking

Drift cells provide a nominal hit position with their drift-time measurements that have a left/right ambiguity on the spatial origin of the ionization. The resolution of this ambiguity is achieved in the reconstruction of the true track using multiple drift-cell hits. DCT events are reconstructed first

with drift times that are converted to two hit positions in the bending view per drift cell following the time( $t$ )-to-distance( $b$ ) relationship. This relationship is simply a constant to first order,  $v$ , known as the drift velocity,  $b = v \times t$ . The  $v$  of ionization electrons is a function of both the gas properties inside the DCT and the electric drift field. The physical properties of the gas will be discussed in the next section. For a proportion of CO<sub>2</sub>-Ar at 90:10 and the electric field of 1.3 kV/cm, the drift velocity is  $b \approx 6$  mm/ $\mu$ s. Higher-order corrections are possible following a distribution of drift times and positions and then integrating. Drift times are recorded after a trigger from the TOF system. Sense wires with above-threshold signals generate a region of interest (ROI) for the ADC to digitize the track-induced pulse. Non-bending-view positions are reconstructed using the charge division method with signals from both ends of the sense wires. An example straight-through (magnet off) muon event is shown on the left of Figure 4 with all 72 drift-cell layers displayed. Each sense-wire drift time from its ROI has been converted to two hit positions.

The staggering of alternating sense wires mentioned above provides a local true track with smaller deviation per hit than the mirrored track. To quantitatively differentiate the true hit for a drift cell, an algorithm based on the Hough transform [8] was developed. Implementing this algorithm saves computational time in comparison to track-fitting methods with unresolved hits. In the Hough transform, each hit Cartesian coordinate ( $x, y$ ) is transformed into the Hough space ( $\theta, r$ ) like  $r = x \cos \theta + y \sin \theta$ , and the inverted Hough transform of a ( $\theta, r$ ) pair of coordinates to ( $x, y$ ) is a line where  $r$  is the displacement of the line from the center of the DCT. The true hit positions are found by performing the Hough transform on all drift-cell bending-view hits and determining the Hough space ( $\theta, r$ ) that the most hits have voted for. This is seen in the transform by constructing a 2-D histogram and binning in ( $\theta, r$ ) and yielding, for the example muon event, the right of Figure 4. There is a clear distinction of two regions in Hough space with many hits voting for common Hough coordinates, where the highest is the true track. Sampling the full range of  $\theta$  allowed in the acceptance of the HELIX instrument and calculating  $r$  resolves the ambiguity. For curved tracks, a circular Hough transform with 3 parameters, adding to ( $\theta, r$ ) the curvature of the track ( $\kappa$ ), is currently under development and testing.

## 5. Housekeeping system

The drift velocity is the parameter governing the drift-time-to-distance conversion, allowing reconstruction, and thereby tracking of cosmic rays. It is dependent on the density and composition of the gas and the electric-field strength, i.e.  $v = f(\rho, E)$ . A housekeeping suite was designed in order to control and record the gas density and field strength. This suite is a subset of the full HELIX housekeeping system, which also includes components for control and monitoring of other subsystems such as the magnet and the RICH. The central component of the DCT housekeeping system is based on a microcontroller, the TM4C123 launchpad from Texas Instruments. This circuit interfaces with all of the housekeeping devices required for proper DCT operation.

As stated, the uniformity of the electric field provides a constant drift velocity. Field-shaping electrodes and drift-field wires are employed to improve uniformity. The electric fields for both are generated by two identical Spellman UM8-40 high-voltage supplies. These supplies provide voltage and current-trip control and monitoring. The DCT housekeeping system interfaces with these supplies utilizing Digital to Analog Converters (DACs) and ADCs at the microcontroller.

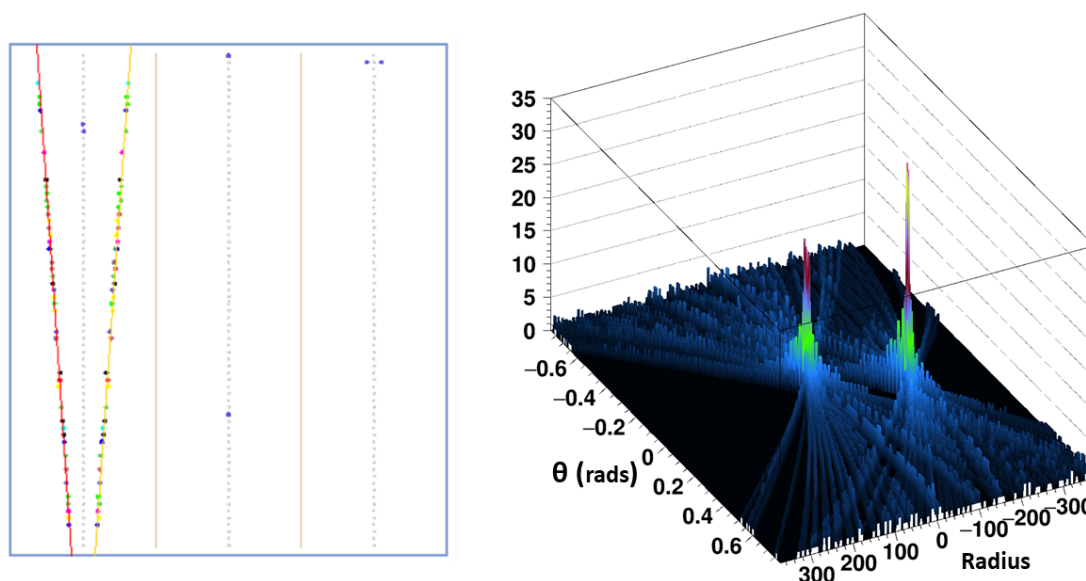


**Figure 4:** **Left:** The bending-view display of a tracker muon event. The gray dots are the sense wires and the orange vertical lines are drift-field wires. Across the top of the display are three drift cells in one layer, and from top to bottom are all 72 layers. There are two sense-wire hits per drift cell, denoted with filled circles of an assortment of colors. **Right:** The 2D mapping of the Hough transform for the muon event at left, where each hit votes for many pairs of Hough space parameters  $(\theta, r)$ . The two best-scoring Hough parameters are inverted to provide the red (best) and yellow lines at left, resolving the correct hit position for each drift cell.

This system provides control and monitoring of the high voltage at the level of 0.1% precision. Multiple components are utilized to control and monitor the density of the gas. The mixing of the gas is performed in-flight by a pair of Alicat Whisper-model flow controllers.  $\text{CO}_2$  and Ar gas are held in canisters that input to flow controllers commanded by the housekeeping PCB. This mixed gas flows through the DCT and out to a third identical flow controller for monitoring of the flow rate during flight,  $\sim 200$  cc/min. The pressure of the gas is held at 1 atm for stability of the gas properties. Pressure transducers monitor the DCT pressure, the high-voltage supplies, and the flow-controller vacuum-reference canister. The high-voltage supplies are housed in a custom pressure vessel with hermetically sealed feedthroughs; the high voltage system is pressurized with the DCT gas to prevent any high-voltage breakdown.

The gas flow provides some temperature uniformity inside the DCT; to further improve the uniformity twenty 2-Watt heater sheets are installed on the four faces of the DCT that do not house the FEEs. The DCT housekeeping system controls each heater individually for fine-tuning of the power. Finally, arrays of thermistors are installed on all DCT faces to precisely measure the temperature profile. This is important to ensure uniformity and inform heater tuning if necessary. There are 23 thermistors distributed over all six faces of the DCT; they provide  $\sim 0.5^\circ\text{C}$  precision. The heaters and thermistors interface with the DCT housekeeping microcontroller. All components of the system have been tested during the HELIX thermal vacuum test in 2022 at the NASA Armstrong Test Facility.

## 6. Conclusions

The DCT system testing, which includes qualifications of the structure and electronic components for flight, has been completed. The data acquisition (DAQ) and housekeeping systems have been developed and implemented, and have been shown to successfully support muon straight-through tracking. Analysis software is currently being developed for curved tracks. The design and stringing, as well as the initial validation of the DAQ, were performed at Indiana University. The DCT system is installed in the magnet bore on the HELIX payload, currently housed at the University of Chicago, where all HELIX subdetectors have been delivered and integrated into the payload. Integration tests of the DAQ have been carried out alongside flight-software development. With multiple successful environment and ground tests carried out since 2020, including a successful thermal-vacuum test of the payload in 2022, the first HELIX flight is expected to take place from Sweden by long-duration balloon in late spring 2024.

## 7. Acknowledgements

This work is supported in the US by grant 80NSSC20K1840 from the National Aeronautics and Space Administration (NASA) and in Canada by grants from the Natural Sciences and Engineering Research Council (NSERC) and the Canadian Space Agency's Flights and Fieldwork for the Advancement of Science and Technology (FAST) program.

## References

- [1] S.P. Wakely et al., *Prospects for High Energy Light Isotope Measurements on Balloons*, in proceedings of the 34th International Cosmic Ray Conference (The Hague), PoS(ICRC2015) 682 (2015).
- [2] S. Coutu et al., *Cosmic-ray isotope measurements with HELIX*, in proceedings of the 35th International Cosmic Ray Conference (Busan), PoS(ICRC2017) 226 (2017).
- [3] M.E. Wiedenbeck et al., *A cosmic-ray age based on the abundance of Be-10* ApJ (1980). doi:10.1086/183310
- [4] P. Allison et al., *The Design and Construction of the HELIX RICH Detector*, in proceedings of the 36th International Cosmic Ray Conference (Madison), PoS(ICRC2019) 152 (2019).
- [5] N. Park et al., *Cosmic-ray isotope measurements with HELIX*, in proceedings of the 37th International Cosmic Ray Conference (Berlin), PoS(ICRC2021) 091 (2021).
- [6] M. Tabata et al., *Developing a silica aerogel radiator for the HELIX ring-imaging Cherenkov system*, in Nuclear Instruments and Methods in Physics Research A, 952, 161879, (2020).
- [7] S. Barwick et al., *The high-energy antimatter telescope (HEAT): An instrument for the study of cosmic-ray positrons* in Nuclear Instruments and Methods in Physics Research A, 400, (1997).
- [8] P. Hough, *Method and Means for Recognizing Complex Patterns*, in U.S. Patent No. 3069654. (1962).